Electronic Supplementary Information

Anisotropic Magnetism in Prussian Blue Analogue Films

Daniel M. Pajerowski [a], *Justin E. Gardner* [b], *Daniel R. Talham** [b], *Mark W. Meisel** [a]

[a] Department of Physics and NHMFL, University of Florida, Gainesville, FL 32611-8440, USA
[b] Department of Chemistry, University of Florida, Gainesville, FL 32611-7200, USA
*E-mail: talham@chem.ufl.edu and meisel@phys.ufl.edu

Abstract: The information contained herein is provided to supplement the work presented in the main paper and includes (1) the FTIR spectra and resulting analyses, (2) the AFM data and analyses that provide thickness and deposition rate information, (3) the magnetization versus magnetic field plot of the ZnCr PBA film, and (4) a figure sketching the deposition procedures.

1. Transmission FTIR Spectra of the PBA films

The transmission FTIR spectra of the PBA films generated from 200 cycles are shown in Fig. S1. The fits were made with Lorentzian lineshapes where the absorbance (*Abs*) in arbitrary units is parameterized, Table 1, by the peak frequency, ω_0, that has a width, *W*, and an area, *A*, such that

$$Abs = \frac{AW}{\pi(W^2 + (\omega - \omega_0)^2)} \quad . \tag{S1}$$

Table S1. Results of fitting FTIR cyanide stretches to Lorentzian lineshapes.

PBA	ω_0 (cm^{-1})	W (cm^{-1})	A (arb. units)
CoCr	2172.6	28.7	5.6
	2134.3	12.1	0.2
NiCr	2175.0	22.1	3.6
	2135.0	42.6	1.3
CuCr	2186.2	25.8	2.3
	2123.2	29.8	2.3
CoFe	2162.5	18.7	2.9
	2124.6	31.0	3.4
	2108.0	26.4	2.4
NiFe	2165.2	19.2	3.3
	2120.3	42.6	0.8
CuFe	2173.9	19.8	2.7
	2100.7	11.2	0.3

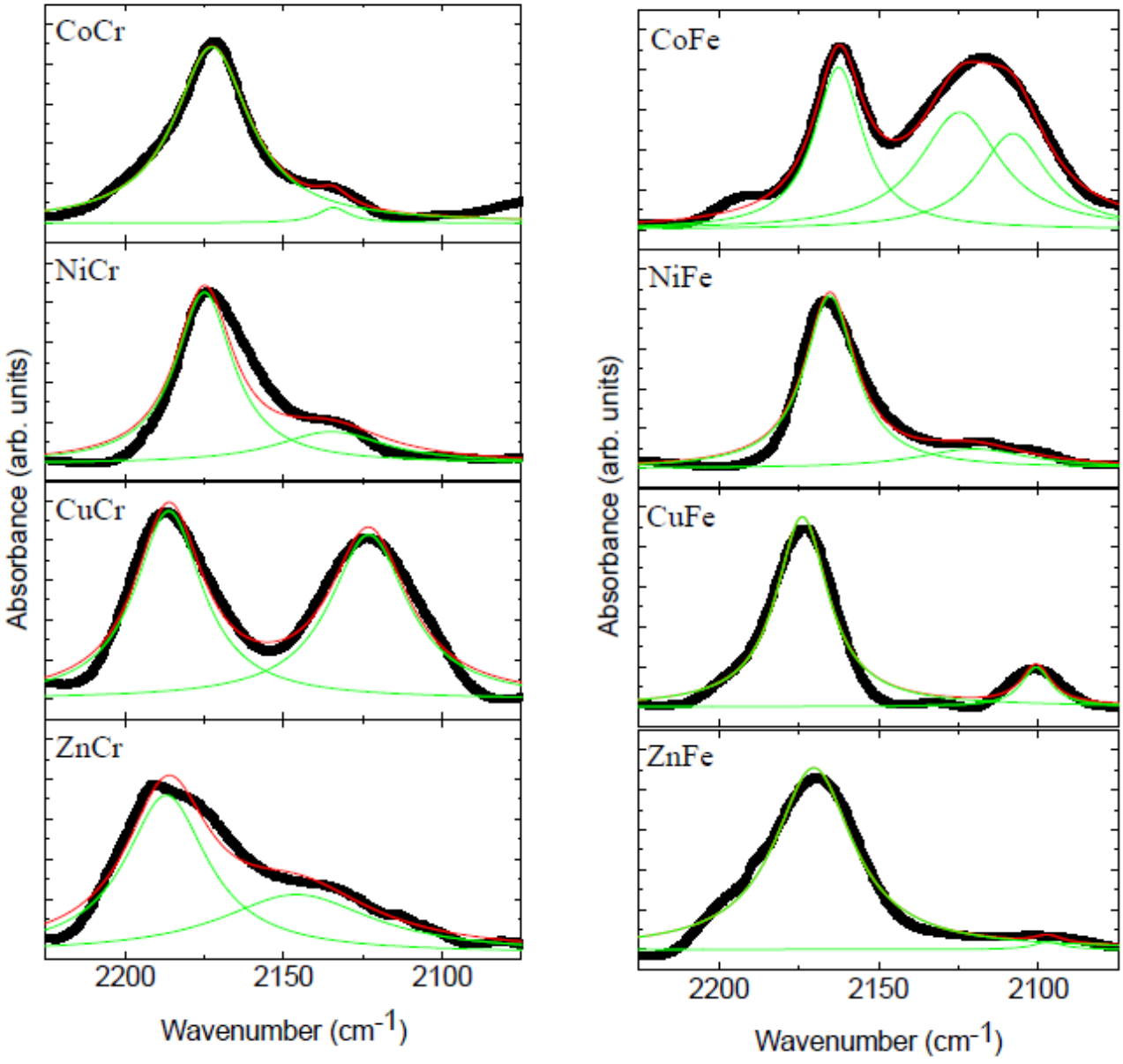

Figure S1. The FTIR spectra (black data points) were fit by different peaks (green lines) whose parameters are listed in Table S1, and the resulting peaks can be summed (red lines, which are sometimes masked by the green lines).

2. Atomic Force Microscopy: Thicknesses and Deposition Rates

Solid supports were cut into squares with sizes of 1 cm^2 and mounted to magnetic disks with double sided tape for AFM analysis. Thickness, roughness, and surface coverage and morphology data were obtained by averaging the measurements of 5 different scans covering areas of 0.01 mm^2. Thickness was determined by inducing a phase boundary in the Prussian blue analog thin films, preventing PBA deposition with a clear acrylic, and measuring the difference in height between the solid support and the surface of the film after the acrylic was removed by solvent, Figs. S2 and S3. The root-mean-square of film height deviation was used to represent the roughness of the films.

Upon the completion of five deposition cycles, uniform substrate coverage with small particulates is achieved for all PBA thin films, except those utilizing Zn as the divalent transition metal ion, Fig. S4. After ten deposition cycles, smooth uniform thin films are observed for the MCr and MFe (M = Co, Ni, and Cu) PBA thin films, and a typical case is shown for the CoFe PBA thin films, Fig. S5. The smooth nature of these films evolves into a rougher surface coverage with added cycles. This rough surface morphology is retained in the PBA thin films while developing even thicker films, see Fig.1 of the main text. The atomic force microscopy (AFM) results on the film thicknesses and roughnesses are summarized in Fig. S6. These data can be fit to smooth lines to extract the deposition rates listed in Table S2.

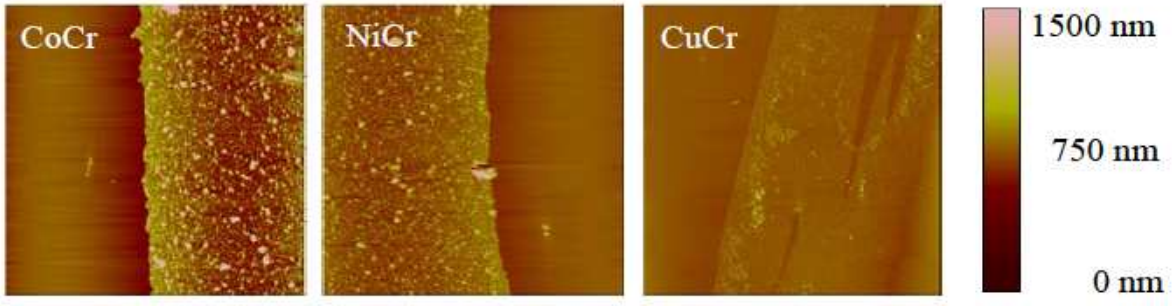

Figure S2. AFM images of 30 cycle $Rb_jM_k[Cr(CN)_6]_l \cdot nH_2O$ thin films synthesized using the sequential deposition method. Uniform coverage and similar surface morphology is observed for CoCr and NiCr. Decreased film thickness (179, 150, and 83 nm) is observed after changing the divalent transition metal site from Co to Ni to Cu. The solid support that was protected by the acrylic, which was subsequently removed, can be seen on the left, right, and left sides of the CoCr, NiCr, and CuCr panels, respectively.

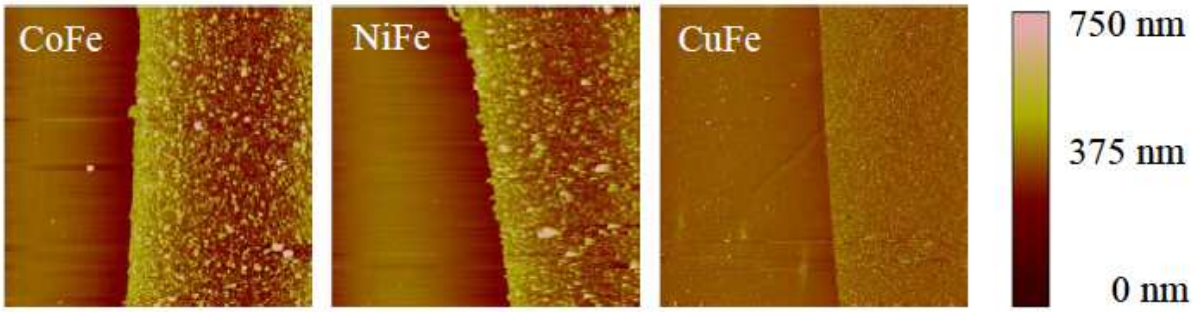

Figure S3. AFM images of 30 cycle $Rb_jM_k[Fe(CN)_6]_l \cdot nH_2O$ thin films synthesized using the sequential deposition method. Uniform surface coverage and similar surface morphology is observed for each film. Decreased film thickness (191, 106, and 81 nm) is observed after changing the divalent transition metal site from Co to Ni to Cu. The solid support that was protected by the acrylic, which was subsequently removed, can be seen on the left side of each panel.

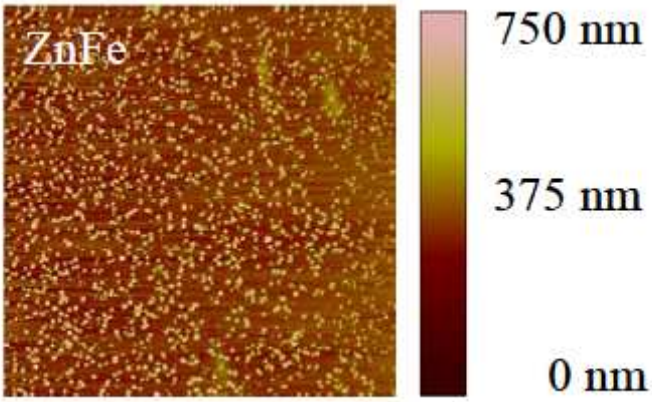

Figure S4. AFM image of a 30 cycle $Rb_{0.5}Zn_{4.0}[Fe^{3+}(CN)_6]_{2.8}[Fe^{2+}(CN)_6]_{0.1} \cdot nH_2O$ thin film synthesized using the sequential deposition method. More deposition cycles did not result in uniform substrate coverage, only increased size of isolated PBA particulates.

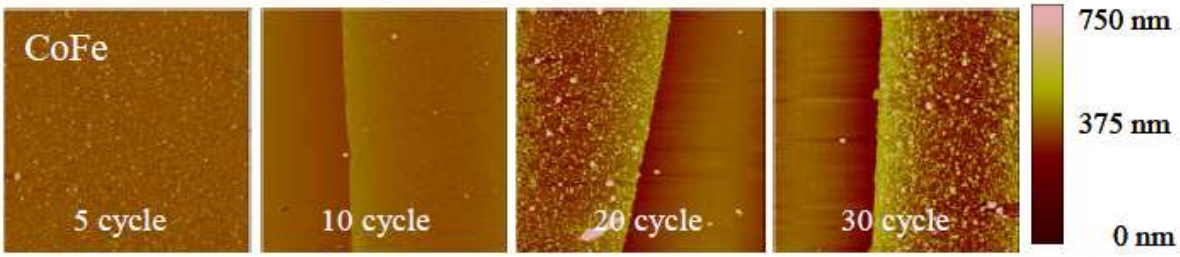

Figure S5. AFM images of $Rb_{0.7}Co_{4.0}[Fe^{3+}(CN)_6]_{2.6}[Fe^{2+}(CN)_6]_{0.2} \cdot nH_2O$ thin films synthesized using the sequential deposition method. Surface coverage is achieved after 5 cycles. The interface between the surface of the solid support, which was protected by acrylic that was removed, and the film is easily seen in the three right panels. The thicknesses are 67, 132, 191, and 325 nm, moving left to right. The surface morphology is maintained throughout film preparation with roughness increasing with increased film thickness.

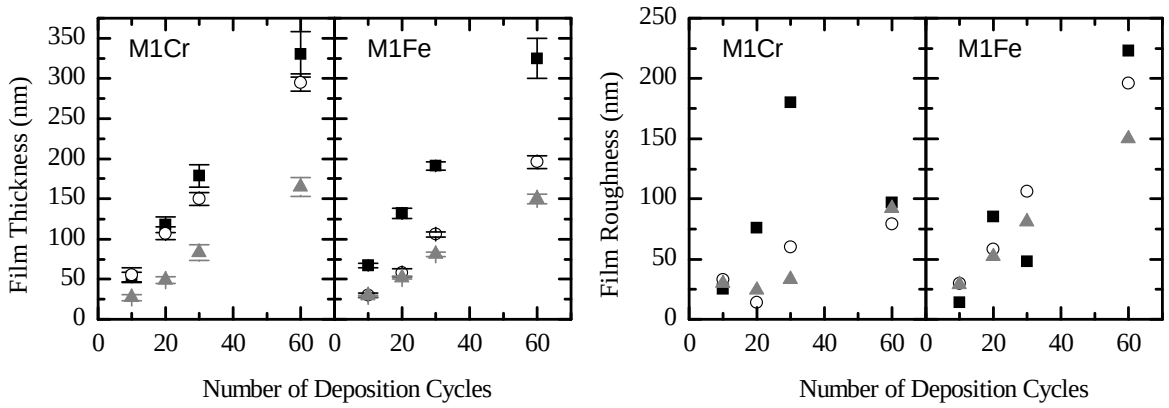

Figure S6. Results of AFM studies. Film thickness (left) and film roughness (right) versus number of deposition cycles are shown for M1 = Co (■), Ni (○), and Cu (▲) divalent metals, with Cr trivalent metals (M1Cr) and Fe trivalent metals (M1Fe). Uncertainty bars on thickness data points represent one standard deviation.

Table S2. Prussian Blue Analogue Film Thickness per Deposition Cycle.

PBA	Nanometers per Cycle
CoCr	5.5 ± 0.5
NiCr	4.8 ± 0.2
CuCr	2.8 ± 0.2
CoFe	5.1 ± 0.3
NiFe	3.4 ± 0.1
CuFe	2.4 ± 0.1

3. Magnetization versus Magnetic Field for the ZnCr PBA Film

The ZnCr and ZnFe PBA films were generated for completeness, as they were expected to be simply diamagnetic since $S_{Zn} = 0$. Indeed, in most instances, the magnetic signals of these samples were significantly masked by the response of the solid support. However, an anisotropic response was detected for the ZnCr PBA film, generated by 200 cycles, at 2 K and in large applied magnetic fields, Fig. S7.

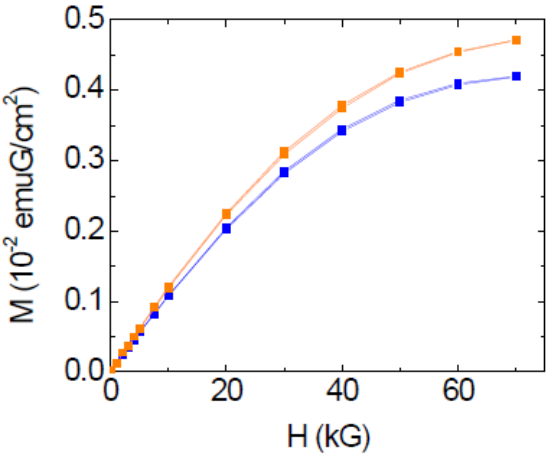

Figure S7. Magnetization of the ZnCr PBA film (200 cycle) versus field. The magnetic field dependences of the low temperature, 2 K, magnetizations are shown when the surface of the film is oriented parallel (■) or perpendicular (■) to the applied magnetic field. Here connecting lines are guides to the eye.

4. Schematic of the Deposition Process

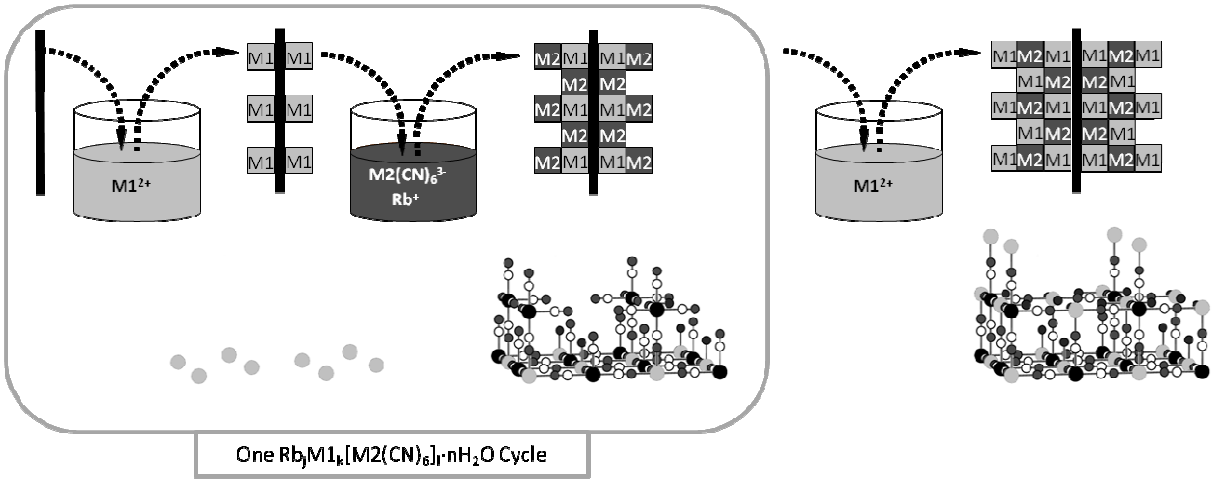

Figure S8. The sequential adsorption technique used to synthesize PBA films. In the upper figures, the dipping process is illustrated, with simplified molecular building blocks. In the lower figures, the layer addition is shown using the constituent M1 (light gray), M2 (black), carbon (white), nitrogen (dark gray), and water (gray) ions to display the Prussian blue crystal structure of the films.